Available online at www.sciencedirect.com

ScienceDirect

Procedia Structural Integrity 13 (2018) 385–390

Structural Integrity Procedia

www.elsevier.com/locate/procedia

ECF22 - Loading and Environmental effects on Structural Integrity

# Micromechanical Modeling of Inter-Granular Localization, Damage and Fracture

Tuncay Yalçinkaya[a,*], İzzet Özdemir[b], Ali Osman Firat[a], İzzet Tarik Tandoğan[a]

[a] *Department of Aerospace Engineering, Middle East Technical University, Ankara 06800, Turkey*
[b] *Department of Civil Engineering, Izmir Institute of Technology, Urla, Izmir 35430, Turkey*

**Abstract**

The recent developments in the production of miniaturized devices increases the demand on micro-components where the thickness ranges from tens to hundreds of microns. Various challenges, such as size effect and stress concentrations at the grain boundaries, arise due to the deformation heterogeneity observed at grain scale. Various metallic alloys, e.g. aluminum, exhibit substantial localization and stress concentration at the grain boundaries. In this regard, inter-granular damage evolution, crack initiation and propagation becomes an important failure mechanism at this length scale. Crystal plasticity approach captures intrinsically the heterogeneity developing due to grain orientation mismatch. However, the commonly used local versions do not possess a specific GB model and leads to jumps at the boundaries. Therefore, a more physical treatment of grain boundaries is needed. For this purpose, in this work, the Gurtin GB model (Gurtin (2008)) is incorporated into a strain gradient crystal plasticity framework (Yalcinkaya et al. (2011), Yalçinkaya et al. (2012), Yalçinkaya (2017)), where the intensity of the localization and stress concentration could be modelled considering the effect of grain boundary orientation, the mismatch and the strength of the GB. A zero thickness 12-node interface element for the integration of the grain boundary contribution and a 10-node coupled finite element for the bulk response are developed and implemented in Abaqus software as user element subroutines. 3D grain microstructure is created through Voronoi tessellation and the interface elements are automatically inserted between grains. After obtaining the localization, the mechanical behavior of the GB is modelled through incorporation of a potential based cohesive zone model (see Park et al. (2009), Cerrone et al. (2014)). The numerical examples present the performance of the developed tool for the intrinsic localization, crack initiation and propagation in micron-sized specimens.


Peer-review under responsibility of the ECF22 organizers.

*Keywords:* Strain Gradient Crystal Plasticity; Cohesive Zone Modeling, Grain Boundary Modeling, Inter-granular Fracture

## 1. Introduction

In the recent years the production of miniaturized products have become a global trend in various industrial clusters such as, electronics, communication, aerospace, biomedical devices, defense and automotive, which requires advanced manufacturing technologies at micron level (see e.g. Yalçinkaya et al. (2017a), Yalçinkaya et al. (2017b)). During plastic deformation of micron-sized metallic products, the material homogeneity assumption does not work anymore.

* Corresponding author. Tel.: +90-312-2104258 ; fax: +90-312-2104250.
*E-mail address:* yalcinka@metu.edu.tr

2452-3216 
Peer-review under responsibility of the ECF22 organizers.
10.1016/j.prostr.2018.12.064

Therefore, crack initiation and propagation are rather dominated by local maximal values around grain boundaries or interfaces (see e.g. Cailletaud et al. (2003), Zhang et al. (2012), Güler et al. (2018)). Our recent experimental studies on Al 6061-T6, using micro DIC technique, illustrated that localization mainly occurs at the grain boundaries under uniaxial tension and at both grain boundaries and grain interiors under equibiaxial tension conditions (Güler et al. (2018)). Most commonly used local crystal plasticity finite element simulations of polycrystalline materials can naturally capture the strain localization evolving due to orientation mismatch. However they lack any kind of grain boundary-dislocation interaction information. On the other hand the non-local (strain gradient) crystal plasticity approaches offer the possibility of defining grain boundary conditions and they can handle the localizations in a much smoother way (see e.g. Yalcinkaya et al. (2011), Yalçinkaya (2013), Klusemann and Yalçinkaya (2013)). However such conditions restrict the physical mechanisms to limiting cases resulting in complete blockage of dislocations or free transition through grain boundaries. Even though it is a considerable improvement for the plasticity modeling at grain scale a special treatment of the grain boundaries is required for more physical simulations. In this context the purpose of the current work is twofold. Firstly, we incorporate a specific grain boundary model (Gurtin (2008)) into a strain gradient crystal plasticity framework (Yalcinkaya et al. (2011), Yalçinkaya et al. (2012)) to simulate the inter-granular localizations in 3D within a more physical context, which has been successfully done before in 2D and for bi-crystal cases (see Özdemir and Yalçinkaya (2014), Özdemir and Yalçinkaya (2017)). Secondly, the inter-granular crack initiation and propagation is obtained through the insertion of potential based cohesive zone elements between the grains (see Park et al. (2009), Cerrone et al. (2014)). All computations are conducted in Abaqus software through UEL files and the developed scripts for the pre- and post-processing procedures. The numerical examples present the performance of the developed tool for the intrinsic localization, crack initiation and propagation in micron-sized specimens.

## 2. Strain Gradient Crystal Plasticity, GB and Cohesive Zone Modeling

For the modelling of the grain boundary behavior two types of user finite element subroutine have been developed and implemented in Abaqus software. The simulation of the size dependent bulk material behavior is conducted through a rate dependent, higher order, plastic slip based, strain gradient crystal plasticity model taking into account plastic slips and displacement as coupled degree of freedom (Yalcinkaya et al. (2011), Yalçinkaya et al. (2012), Yalçinkaya (2017)). The model is based on the additive decomposition of the strain into elastic and plastic components and the plastic slip field evolution is governed by $\dot{\gamma}^\alpha = \dot{\gamma}_0^\alpha \left(|\tau^\alpha + \nabla \cdot \xi^\alpha| / s^\alpha\right)^{\frac{1}{m}} \operatorname{sign}(\tau^\alpha + \nabla \cdot \xi^\alpha)$ where $\tau^\alpha = \sigma : \mathbf{P}^\alpha$ is the resolved Schmid stress on the slip systems with $\mathbf{P}^\alpha = \frac{1}{2}(\mathbf{s}^\alpha \otimes \mathbf{n}^\alpha + \mathbf{n}^\alpha \otimes \mathbf{s}^\alpha)$, the symmetrized Schmid tensor, where $\mathbf{s}^\alpha$ and $\mathbf{n}^\alpha$ are the unit slip direction vector and unit normal vector on slip system $\alpha$, respectively and $\xi^\alpha$ is the micro-stress vector $\xi^\alpha = \partial \psi_{\nabla\gamma} / \partial \nabla \gamma^\alpha = A \nabla \gamma^\alpha$ bringing the plastic slip gradients into the plasticity formulation. $A$ is a scalar quantity, which includes an internal length scale parameter, and in this work it is defined as $A = ER^2/(16(1-\nu^2))$ where $R$ is a typical length scale for dislocation interactions.

The simulation of the grain boundary behavior is conducted through the Gurtin GB model (see e.g. Gurtin (2008)) which considers the effect of the grain boundary orientation and the orientation mismatch between neighboring grains. The slip incompatibility of the neighboring grains is described in terms of the grain boundary Burgers tensor defined as, $\boldsymbol{G} = \sum_\alpha [\gamma_B^\alpha \boldsymbol{s}_B^\alpha \otimes \boldsymbol{n}_B^\alpha - \gamma_A^\alpha \boldsymbol{s}_A^\alpha \otimes \boldsymbol{n}_A^\alpha](\boldsymbol{N}\times)$ where for any vector $\boldsymbol{N}$, $\boldsymbol{N}\times$ is the tensor with components $(\boldsymbol{N}\times)_{ij} = \varepsilon_{ikj} N_k$. In this relation, the relative mis-orientation of grains is reflected by the difference term and the grain boundary orientation is accounted for by the tensor $\boldsymbol{N}\times$. $C_{AA}^{\alpha\beta}$ and $C_{BB}^{\alpha\beta}$ represent interactions between slip systems within grain A and grain B respectively, whereas $C_{AB}^{\alpha\beta}$ represent the interaction between slip systems of the two grains and called inter-grain interaction moduli. Ignoring the dissipative effects, a simple potential energy in the form $\psi_{GB} = \frac{1}{2}\kappa |\boldsymbol{G}|^2$ is used where $\kappa$ is a positive constant modulus and it represents the strength of the grain boundary. Principal of virtual power is followed for both bulk and grain boundary parts, where the rate of free energy expressions are used. Then dissipation inequalities are obtained for both parts. Obtained balance equations and grain boundary relations are solved through the finite element method.

For the cohesive zone modeling the element formulation from (Park et al. (2009)) is employed, which gives the following traction-separation relation,

$$T_n(\Delta_n, \Delta_t) = \frac{\Gamma_n}{\delta_n}\left[ m\left(1-\frac{\Delta_n}{\delta_n}\right)^\alpha \left(\frac{m}{\alpha}+\frac{\Delta_n}{\delta_n}\right)^{m-1} - \alpha\left(1-\frac{\Delta_n}{\delta_n}\right)^{\alpha-1}\left(\frac{m}{\alpha}+\frac{\Delta_n}{\delta_n}\right)^m \right] \times \left[ \Gamma_t\left(1-\frac{|\Delta_t|}{\delta_t}\right)^\beta \left(\frac{n}{\beta}+\frac{|\Delta_t|}{\delta_t}\right)^n + \langle \Phi_n - \Phi_t \rangle \right]$$

$$T_t(\Delta_n,\Delta_t)=\frac{\Gamma_t}{\delta_t}\left[n\left(1-\frac{|\Delta_t|}{\delta_t}\right)^{\beta}\left(\frac{n}{\beta}-\frac{|\Delta_t|}{\delta_t}\right)^{n-1}-\beta\left(1-\frac{|\Delta_t|}{\delta_t}\right)^{\beta-1}\left(\frac{n}{\beta}+\frac{|\Delta_t|}{\delta_t}\right)^{n}\right]\times\left[\Gamma_n\left(1-\frac{\Delta_n}{\delta_n}\right)^{\alpha}\left(\frac{m}{\alpha}+\frac{\Delta_n}{\delta_n}\right)^{m}+\langle\Phi_n-\Phi_t\rangle\right]\frac{\Delta_t}{|\Delta_t|}$$

where $m,n$ are non-dimensional exponents, $T_n$ is the normal cohesive traction, $T_t$ is the tangential cohesive traction, $\alpha,\beta$ are shape parameters, $\lambda_n,\lambda_t$ are initial slope indicators, $\Gamma_n,\Gamma_t$ are energy constants, $\Delta_n$ is the normal separation, $\Delta_t$ is the effective sliding displacement, $\delta_t,\delta_n$ are the normal and tangential final crack opening widths, $\Phi_n,\Phi_t$ are fracture energies. For more details about the model see (Park et al. (2009)). Abaqus input files including the geometry, mesh, loading, solid elements, grain boundary elements and the cohesive elements are prepared through developed scripts and the interface elements are inserted between the grains automatically. In the following, two different types of numerical analysis considering the grain boundary model and cohesive zone approach are presented for the illustration of inter-granular localization, crack initiation and propagation.

## 3. Numerical Examples

A mixed finite element formulation is used for the solution of the strain gradient crystal plasticity problem inside each grain. The displacement and plastic slips are taken as primary variables and these fields are determined within the problem domain by solving simultaneously the linear momentum balance and the microscopic force balance. The discretization is conducted by 10-node tetrahedra elements with quadratic interpolation for the displacement field and linear interpolation for the slips. To facilitate the integration of the grain boundary model contributions, 12-node zero thickness interface elements are developed and inserted along the grain boundaries. By means of these elements, one has the access to the slip values along the grain boundary as approached from grain A and grain B. Initially the interface elements do not possess any kind of mechanical cohesive behavior and does not cause discontinuity in displacement field. In the solution phase, the displacement continuity across the grain boundary is fulfilled by means of equality constraints (rigid ties) enforcing the same displacement field for the corresponding nodes of on the two sides of an interface element. Later on, mechanical cohesive behavior is obtained through the insertion of potential based cohesive zone elements (Cerrone et al. (2014)) between the grains.

First, we consider a cylindrical specimen having length of 100 $\mu$m and diameter 25 $\mu$m and analyze both microscopic and macroscopic responses considering the grain boundary model under 5% uniaxial loading. The specimen includes 50 randomly oriented grains and the material parameters are presented in Table 1.

Table 1: Material properties of the strain gradient crystal plasticity model.

| Young modulus E [MPa] | Poisson ratio $\nu$ [/] | Reference slip rate $\dot{\gamma}_0$ [s$^{-1}$] | Slip resistance s [MPa] | Orientations [°] | Material length scale $R$ [$\mu$m] |
|---|---|---|---|---|---|
| 70000.0 | 0.33 | 0.115 | 25.0 | Random | 0.4 |

Our purpose here is to illustrate the effect of the grain boundary strength on the microstructure evolution and the macroscopic stress-strain response. with different $\kappa$ values. For this reason the stress distribution in the loading direction is plotted in Figure 1 for $\kappa=0,1,3,5$ values. As the $\kappa$ value is increased from 0 to high values the grain boundary behavior moves from soft (micro free) to hard (zero slip) and the stress concentrations at the grain boundaries increases as shown in Figure 1. An increase in $\kappa$ also results in more hardening in the macroscopic engineering stress-strain response (see Figure 2). When there is no mis-orientation between the grains, no matter what value of $\kappa$ is used there is no affect of grain boundary. $\kappa$ amplifies the effect of mis-orientation. In Figure 2 the macroscopic response for the case where the random orientation set for the Euler angles is constrained $(40^\circ-45^\circ)$ which results in a much stronger response and the effect of $\kappa$ is reduced due to the decreased mis-orientation between the grains.

In the next example the response of the microstructure for the crack initiation and propagation is addressed. The fracture energies $(\Phi_n,\Phi_t)$ and the maximum stress values $(\sigma_{max},\tau_{max})$ are identified as 60N/m and 0.06MPa respectively. The initial slope indicators $(\lambda_n,\lambda_t)$ and shape parameters $(\alpha,\beta)$ are taken as 0.005 and 2 respectively. Three

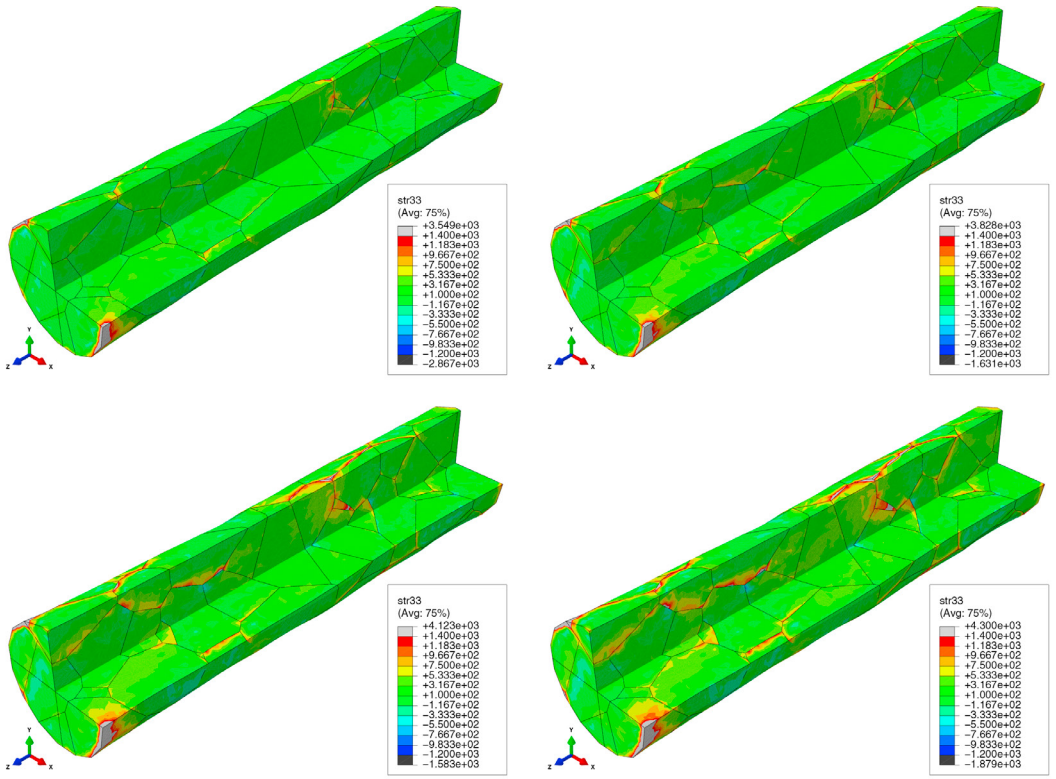


Fig. 1: Stress distribution for $\kappa = 0$ (upper-left), $\kappa = 1$ (upper-right), $\kappa = 3$ (lower-left) and $\kappa = 5$ (lower-right) values of the grain boundary strength.

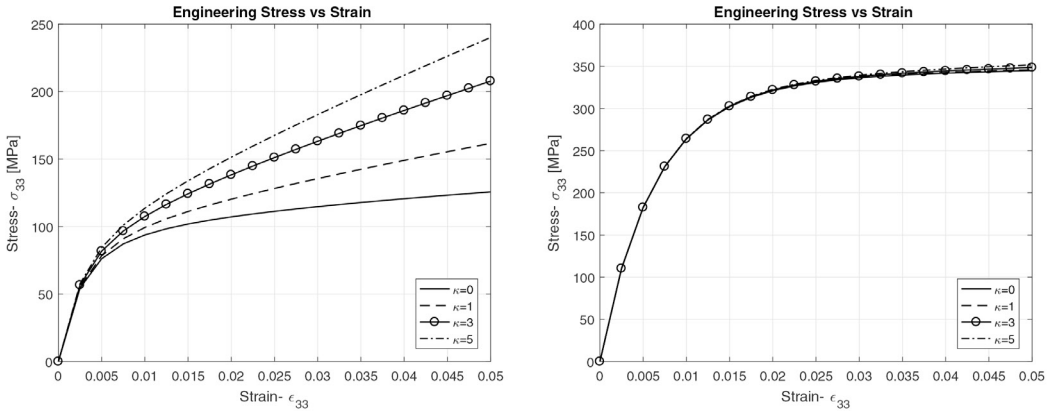


Fig. 2: Stress vs strain response for different $\kappa$ values: (i) for random orientations (left), (ii) for grains with limited mis-orientation (right).

different randomly oriented grain sets are considered in the numerical analysis to illustrate the effect of the microstructural anisotropy on the crack initiation. By coincidence the crack initiation for the first two sets are the same (see Figure 3), which is a favorable location due to the grain boundary orientation with respect to loading. However, the location of the crack initiation alters for the set 3 due to the major change in the Euler angles of the crystal orientation. In Figure 4 the force-displacement response of the micro-structures are presented. In addition to the three different

micro-structures the textured case in the previous analysis is also presented in the same figure. A strong anisotropy effect is observed in both local and macroscopic responses. The orientation set of the example in the grain boundary model and the orientation set 1 in the cohesive zone example are identical. A closer look would reveal that the spatial evolution is quite similar in both cases. In GB model $\kappa$ allows to identify the intensity of localization, yet it is not enough alone for the simulation of the crack initiation/propagation. Even though the models are used separately here, the combination of both models is required for a physics based localization, crack incitation/propagation simulations of micron sized polycrystalline materials.

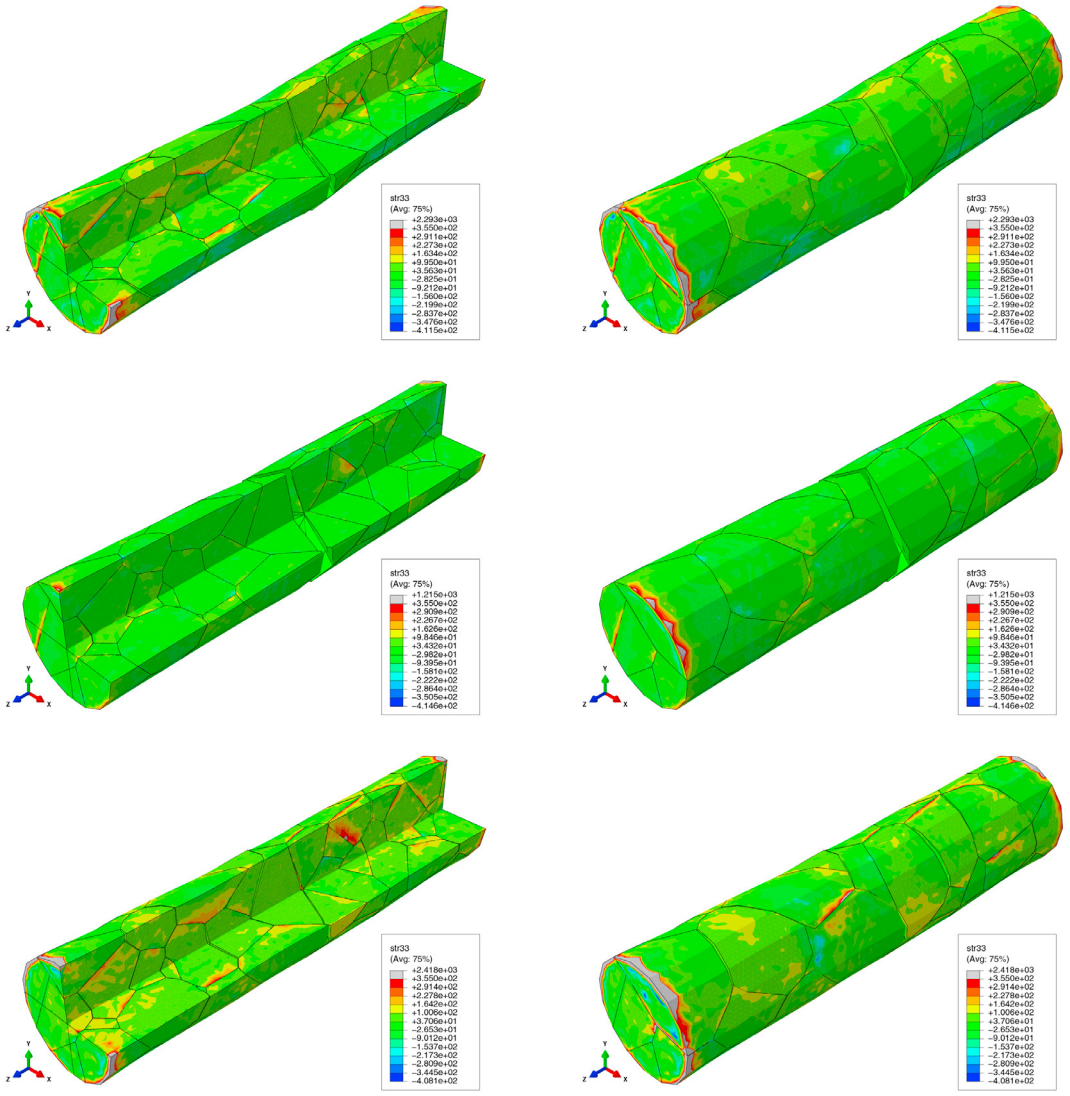


Fig. 3: Crack initiation location for the orientation set 1 (top), orientation set 2 (middle) and set 3 (bottom).

## 4. Conclusion and outlook

This paper addresses the evolution of plastic microstructure in micron-sized polycrystalline specimens through a strain gradient crystal plasticity framework. The mis-orientation and GB-orientation dependent intergranular local-

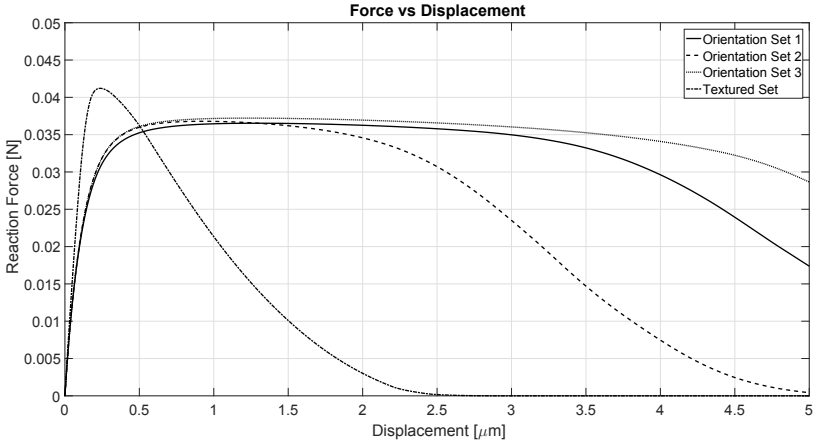


Fig. 4: Force-displacement response for different orientation sets.

ization is studied through a grain boundary model representing the coarse grained representation of complex grain boundary-dislocation slip interaction mechanisms. The initiation and propagation of the inter-granular cracks are simulated by cohesive zone elements. The current study includes only a virtual polycrystalline created by Voronoi and the results are not compared with any experimental data yet. But it presents a great potential for the modeling of plasticity, damage and fracture in small specimens as it is one of the rare studies incorporating GB and CZ models into a strain gradient polycrystalline plasticity framework.

## References

Cailletaud, G., Forest, S., Jeulin, D., Feyel, F., Galliet, I., Mounoury, V., Quilici, S., 2003. Some elements of microstructural mechanics. Comp. Mater. Sci. 27, 351–374.

Cerrone, A., Wawrzynek, P., Nonn, A., Paulino, G.H., Ingraffea, A., 2014. Implementation and verification of the parkpaulinoroesler cohesive zone model in 3d. Eng. Fract. Mech. 120, 26–42.

Güler, B., Simsek, Ü., Yalçinkaya, T., Efe, M., 2018. Grain-scale investigations of deformation heterogeneities in aluminum alloys. AIP Conf. Proc. 1960, 170005.

Gurtin, M.E., 2008. A theory of grain boundaries that accounts automatically for grain misorientation and grain-boundary orientation. J. Mech. Phys. Solids 56, 640–662.

Klusemann, B., Yalçinkaya, T., 2013. Plastic deformation induced microstructure evolution through gradient enhanced crystal plasticity based on a non-convex helmholtz energy. Int. J. Plasticity 48, 168–188.

Özdemir, I., Yalçinkaya, T., 2014. Modeling of dislocationgrain boundary interactions in a strain gradient crystal plasticity framework. Comput. Mech. 54, 255–268.

Özdemir, I., Yalçinkaya, T., 2017. Strain gradient crystal plasticity: Intergranular microstructure formation. Handbook of Nonlocal Continuum Mechanics for Materials and Structures 1, 1–29.

Park, K., Paulino, G.H., Roesler, J.R., 2009. A unified potential-based cohesive model of mixed-mode fracture. J. Mech. Phys. Solids 57, 891–908.

Yalçinkaya, T., 2013. Multi-scale modeling of microstructure evolution induced anisotropy in metals. Key Eng. Mater. 554, 2388–2399.

Yalçinkaya, T., 2017. Strain gradient crystal plasticity: Thermodynamics and implementation. Handbook of Nonlocal Continuum Mechanics for Materials and Structures 1, 1–32.

Yalçinkaya, T., Brekelmans, W.A.M., Geers, M.G.D., 2012. Non-convex rate dependent strain gradient crystal plasticity and deformation patterning. Int. J. Solids Struct. 49, 2625–2636.

Yalçinkaya, T., Demirci, A., Simonovski, I., Özdemir, I., 2017a. Micromechanical modelling of size effects in microforming. Procedia Eng. 207, 998–1003.

Yalçinkaya, T., Özdemir, I., Simonovski, I., 2017b. Micromechanical modeling of intrinsic and specimen size effects in microforming. Int. J. Mater. Form. doi:10.1007/s12289-017-1390-3.

Yalcinkaya, T., Brekelmans, W.A.M., Geers, M.G.D., 2011. Deformation patterning driven by rate dependent non-convex strain gradient plasticity. J. Mech. Phys. Solids 59, 1–17.

Zhang, P., Karimpour, M., Balint, D., Lin, J., 2012. Cohesive zone representation and junction partitioning for crystal plasticity analyses. Int. J. Numer. Meth. Eng. 92, 715–733.